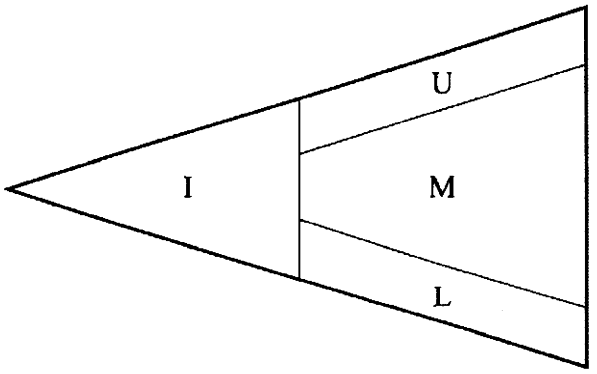

Fig. 2. Separation of meniscus regions. Anterior horn segment of meniscus was divided into inner (I), and outer halves, and the latter was further divided into upper surface (U), middle (M), and lower surface (L) regions. Gene expression was evaluated in those regions respectively. Cross-section of a meniscus is shown.

explants were rinsed three times with ice-cold phosphate-buffered saline (PBS). The samples were stored at −20 °C until use.

To determine the rate of [^{3}H]proline incorporation, the explants were minced and digested with proteinase K (2 mg/ml; Sigma, St. Louis, Missouri) at 58 °C for 48 h. After digestion, the samples were centrifuged and radioactivity of the supernatant was measured. The radioactivity was normalized by DNA content, which was determined by Quant-iT PicoGreen dsDNA assay kit (Invitrogen, Carlsbad, California).

Transmission electron microscopy

Three pairs of OA menisci and three pairs of control menisci were used for the evaluation. For the analysis, the tissues were obtained as thin slices from the anterior horn segments, which were immediately immersed in 2.5% glutalaldehyde in the cacodylate buffer. The samples were then treated with 1% OsO_4 in cacodylate buffer, dehydrated in graded concentration of ethanol, and embedded in epon with careful attention to the orientation. Sections were cut at 90 nm thickness and stained sequentially with 0.2% oolong tea extract (Nisshin EM, Tokyo, Japan), aqueous uranyl acetate, and lead citrate. The sections were observed under a JOEL JEM-2000 FX-II electron microscope (Nihon Denshi, Tokyo, Japan).

Quantitative image analysis of collagen fibrils was performed following a previously described method[22] with some modifications. In brief, three to five photomicrographs were taken on each section at the magnification of ×20,000, and on each photo, the number and diameters of collagen fibrils were determined using an image analysis software (ImageJ version 1.42e; National Institute of Health, Bethesda, Maryland). For each meniscus, mean fibril diameter, number of fibrils per μm^2, and percentage of the area occupied by fibrils were determined.

Table I
Primer and probe sequences used for quantitative PCR

Gene	Primer and probe sequence	T_m
COL1A1	Forward: 5′-AGCCTGGGGCAAGACAGTGATT-3′	60
	Reverse: 5′-TTGCTTGTCTGTTTCCGGGTTG-3′	
COL1A2	Forward: 5′-ATGAGGAGACTGGCAACCTGAAAAA-3′	58
	Reverse: 5′-TCCAAAGGTGCAATATCAAGGAAGG-3′	
COL2A1	Forward: 5′-GACATAGGAGGGCCCGAGCA-3′	60
	Reverse: 5′-CGGCACCTGAAGGGAGGTCT-3′	
COL3A1	Forward: 5′-TCGAACACGCAAGGCTGTGAG-3′	60
	Reverse: 5′-TGTCGGTCACTTGCACTGGTTGA-3′	
ACAN	Forward: 5′-GCACGAGAAGGGCGAGTGGA-3′	60
	Reverse: 5′-GCTCCTGGGCTCAGCGTCCT-3′	
*IGF1**	Forward: 5′-GTACTTCAGAAGCAATGGGAAA-3′	56
	Reverse: 5′-GTTGAAATAAAAGCCCCTGTCT-3′	
	Probe Flu: 5′-GTGAAGATGCACACCATGTCCTCCTCG-3′	
	LC: 5′-ATCTCTTCTACCTGGCGCTGTGCCTGC-3′	
PDGFA	Forward: 5′-TCATTTACGAGATTCCTCGG-3′	58
	Reverse: 5′-TGCTCCTCTAACCTCACCTG-3′	
PDGFB	Forward: 5′-GGAAGAAGCCAATCTTTAAGAAG-3′	58
	Reverse: 5′-CTTCAGTGCCGTCTTGTCAT-3′	
TGFB1	Forward: 5′-ATGTTCTTCAACACATCAGAGC-3′	58
	Reverse: 5′-GGTGACATCAAAAGATAACCAC-3′	
GAPDH	Forward: 5′-AAAACCTGCCAAATATGATGAC-3′	58
	Reverse: 5′-CAGGAAATGAGCTTGACAAAGT-3′	
ACTB	Forward: 5′-ATTAAGGAGAAGCTGTGCTACGTC-3′	58
	Reverse: 5′-ATGATGGAGTTGAAGGTAGTTTCG-3′	

COL1A1, collagen, type I, alpha 1; *COL1A2*, collagen, type I, alpha 2; *COL2A1*, collagen, type II, alpha 1; *COL3A1*, collagen, type III, alpha 1; *ACAN*, aggrecan; *IGF1*, insulin-like growth factor 1; *PDGFA*, platelet-derived growth factor alpha polypeptide; *PDGFB*, platelet-derived growth factor beta polypeptide; *TGFB1*, transforming growth factor, beta1; *GAPDH*, glyceraldehyde-3-phsophate dehydrogenase; *ACTB*, actin, beta.

* Hybridization probes were used for quantitative PCR. Flu: probe conjugated with Fluorescein; LC: probe conjugated with LC640.

Biomechanical measurement

Six pairs of lateral and medial OA menisci and six pairs of control menisci were used for this analysis. For measurement, two to four cylindrical specimens, 4 mm in diameter, were harvested from the anterior horn segment of each meniscus. Those specimens were acquired along the periphery of the menisci, 1–2 mm inside from the outer margin, in a side-by-side manner. The number of obtained specimens varied among the menisci depending on the size and the severity of degeneration (when present). The specimens were prepared perpendicular to the tibial (lower) surface using a core reamer. After the acquisition, the upper part of the specimen was cut parallel to the tibial surface so that it would be 3 mm in height. Prior to the measurement, a wet weight of the specimen was determined.

Uniaxial confined compression test was performed according to a previously described method[23]. Each specimen was placed with the tibial surface facing down into a 4.0 mm diameter × 30 mm deep well in an acrylic chamber upon a porous filter. The chamber was then immersed in physiological saline in a reservoir, and the measurement was performed while the specimen was submerged in the saline. Compression load was applied to the specimen by a compression testing machine (Model SV-201NA, Imada Seisakusyo, Aichi, Japan). For measurement, a 4.0-mm diameter stainless indenter was gently inserted into the well in the acrylic chamber onto the specimen, and a constant load of 2 g was applied initially for 15 min as preloading. The load was then suddenly increased to 10 g, and the linear displacement rate was measured at 12 time points between 1 and 5000 s after the increase of the load. The applied load was maintained at 10 g throughout the measurement, which was monitored continuously with a load cell (Model LC-050N, Imada Seisakusyo). Two parameters, aggregate modulus (solid component stiffness) and permeability (measure of fluid flow through the tissue), which characterize the viscoelastic nature of the meniscus, were calculated using a nonlinear least squares optimization algorithm incorporating linear biphasic theory[24]. After biomechanical evaluation, the specimen was completely dried in a vacuum dryer and the dry weight was determined. Water content of the specimen was defined as the percentage of the weight lost by drying relative to that of the wet weight. Aggregate modulus, permeability, and water content were compared between OA and control menisci.

Statistics

Statistical significance of the data was evaluated using analysis of variance (ANOVA), and Fischer's Protected Least Significant Difference (PLSD) was used as a post-hoc test when necessary. Two-tailed *P*-values less than 0.05 were considered significant.

Results

Macroscopic observation

In control menisci, the anatomical shape was well preserved in all samples [Fig. 1(A)]. They had smooth surfaces and did not show macroscopic signs of degeneration except for the presence of slight fraying of the inner margin of the medial meniscus of four samples. For OA menisci, macroscopic appearance differed obviously between lateral and medial menisci. Since all OA menisci were obtained from medially involved knees, medial menisci underwent overt degenerative changes, while lateral menisci preserved the anatomical shape with few signs of macroscopic degeneration [Fig. 1(B)]. The changes of the medial menisci were most notable in the body and posterior horn segments, where the matrix was lost or severely fibrillated. Even in such menisci, the anterior horn segment was preserved well, showing few signs of matrix loss or degeneration.

Histological evaluation

The hematoxylin and eosin stained sections of the control lateral menisci showed short, thick wedge-shaped sections with smooth surfaces [Fig. 3(A) and (B)]. The inner area was filled with densely packed fibril bundles, and the cells were located sparsely throughout the menisci. In OA lateral menisci, fibril bundles tended to be obscure in the upper and lower surface regions, but the bundle structure was well preserved in the inner area away from the surfaces [Fig. 3(C) and (D)]. The cell density was similar to that in the controls.

Sections from control medial menisci showed a thinner, wedge-shaped cross-section with smooth surfaces [Fig. 3(E) and (F)]. Within the menisci, fibril bundles were densely packed and regularly aligned, resembling that of control lateral menisci. Meniscus cells were located sparsely, and the cell density was similar throughout the section. In medial menisci, changes with OA were more obvious than those in lateral menisci. Sections of OA medial menisci tended to be thicker than the controls, and the fibril bundles were not clearly recognized in the surface regions [Fig. 3 (G) and (H)]. In those regions, cell clusters were occasionally found. Structural change was also noticed in the inner areas, where fibril bundles were coarsely and unevenly distributed. Despite these changes, again, the cell density in OA medial menisci was similar to that of the controls.

Obvious wearing and fraying of fibril bundles was seen in the degenerated areas of OA medial menisci [Fig. 3(I) and (J)]. Even in such severely degenerated regions, cell density did not differ much from that of the controls, and cell clusters were found only occasionally.

Evaluation of matrix gene expression

Next, the expression of mRNA for matrix molecules that constitute menisci was evaluated. For this analysis, menisci were divided into inner, upper surface, middle, and lower surface regions (Fig. 2), and mRNA expression was determined in respective regions.

Considering primary components of menisci[3–11], expression of five matrix genes (*COL1A1*, *COL1A2*, *COL2A1*, *COL3A1* and *ACAN*) was evaluated in this study. First, the expression of two genes encoding type I procollagen (*COL1A1* and *COL1A2*) was evaluated. In control menisci, these genes were expressed at similar low levels in both lateral and medial menisci [Fig. 4(A) and (B)]. In OA menisci, the expression of these genes was dramatically increased in all four regions. The increase was 9- to 52-fold depending on the regions. While the expression of *COL1A1* was equally enhanced in lateral and medial OA menisci [Fig. 4(A)], *COL1A2* expression tended to be more enhanced in medial OA menisci [Fig. 4(B)]. As a consequence, in OA medial menisci, the expression ratios between *COL1A2* and *COL1A1* were significantly higher than those of the control medial menisci [Fig. 4(C)].

The expression of type II procollagen (*COL2A1*) was also enhanced in OA menisci in all four regions [Fig. 4(D)], although the level of increase was lower than that for type I procollagen genes (3- to 19-fold vs 9- to 52-fold).

Among the five genes evaluated, type III procollagen (*COL3A1*) was the one whose expression was most enhanced in OA menisci [Fig. 4(E)]. The increase reached as high as 400-fold. Similar to *COL1A2*, the expression of *COL3A1* tended to be more promoted in medial OA menisci than in lateral OA menisci.

In contrast to *COL3A1*, the increase of aggrecan (*ACAN*) expression in OA menisci was the least among the five genes, which never exceeded 2-fold [Fig. 4(F)].

Because the increase of gene expression in OA menisci was so dramatic, we repeated gene expression analysis of several samples using *ACTB* as an internal control. The result of this analysis confirmed the validity of the above results based on *GAPDH* expression (data not shown).

Expression of possible anabolic factors in OA menisci

In order to elucidate the mechanism(s) for enhanced matrix gene expression in OA menisci, a preliminary experiment was performed to investigate the expression of growth factor genes which could enhance anabolic activity of meniscal fibroblasts. We compared the expression of IGF-1 (*IGF1*), platelet growth factor (PDGF)-A (*PDGFA*), PDGF-B (*PDGFB*), and transforming growth factor (TGF)-β1 (*TGFB1*) between OA and control menisci, and found that the expression of *IGF1*, *PDGFA* and *PDGFB* was increased in OA menisci, while that of *TGFB1* was reduced [Fig. 5(A)–(D)]. Among these three genes, the increase in expression was most obvious with *IGF1*, which reached as high as 50-fold increase. The expression of *IGF1* tended to be higher in medial OA menisci than in lateral OA menisci, though this difference was not statistically significant. The expression of IGF-1 by OA meniscal cells was confirmed at the protein level by immunohistochemistry [Fig. 5(E) and (F)].

Evaluation of collagen neosynthesis

We next evaluated the rate of collagen neosynthesis in OA and control menisci by incorporation of [^{3}H]proline into meniscal explants. Collagens are the primary components of menisci that account for more than 75% of their dry weight[25,26]. Thus, the amount of incorporated [^{3}H]proline should represent the synthetic activity of meniscal cells. In control menisci, incorporation rate of [^{3}H]proline was similar between lateral and medial menisci (Table II). In OA menisci, the incorporation was increased above the control levels. However, the level of increase was rather low compared with the marked increase of procollagen mRNA expression in OA menisci. Because of the limited level of increase and a large variation among the samples, the increase of proline incorporation in OA menisci did not reach the level of significance in either lateral or medial OA menisci.

Ultrastructural evaluation

In order to study the change of meniscal matrix in depth, collagen fibril ultrastructure was evaluated by transmission electron microscopy. This observation was performed on the meniscal tissues obtained from the middle regions of the anterior horn segments (Fig. 2).

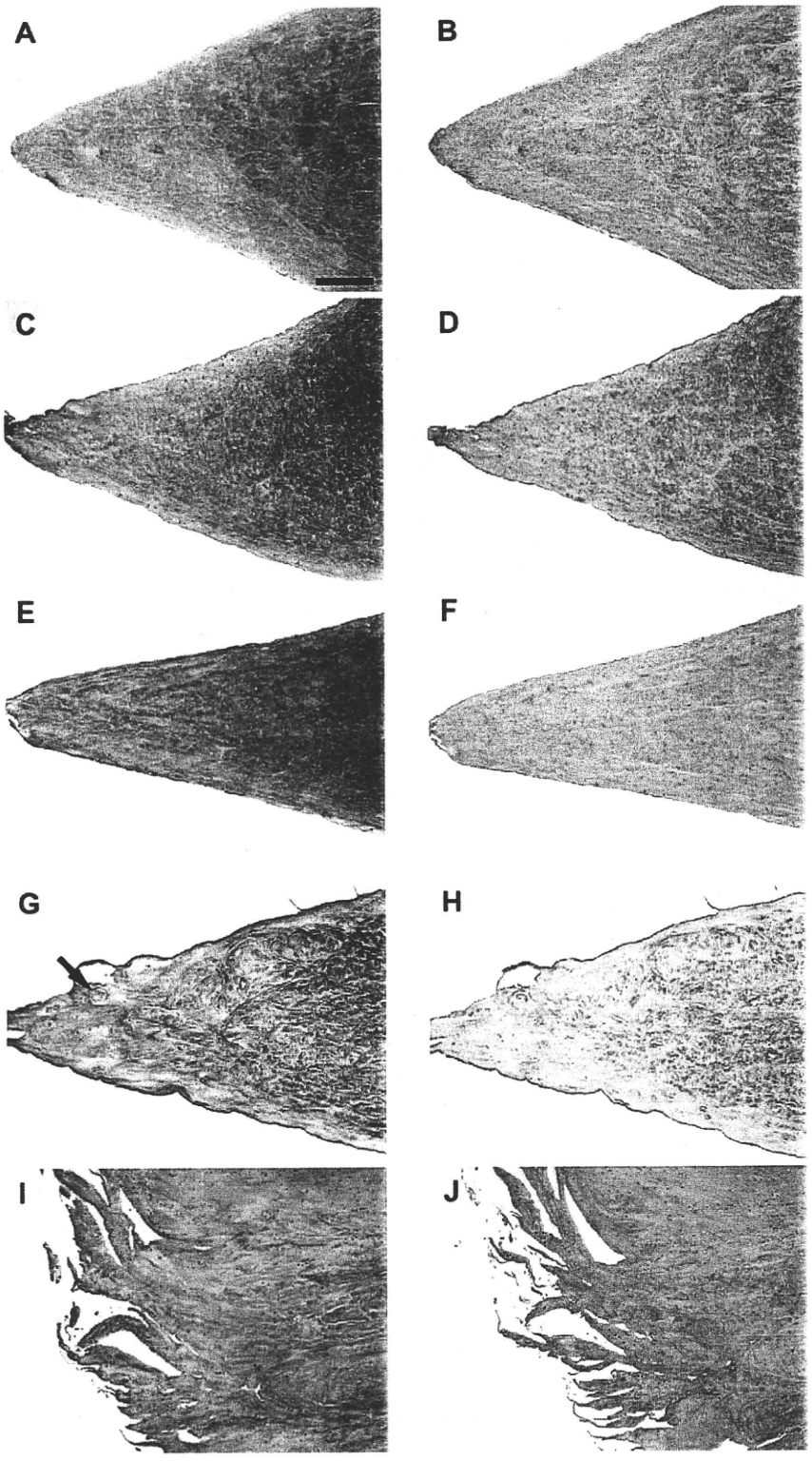

Fig. 3. Histology of OA and control menisci. Photomicrographs of sections from the anterior horn segments of control (A and B) and OA lateral menisci (C and D), and control (E and F) and OA medial menisci (G and H) are shown together with those from a degenerated area in the body segment of OA medial meniscus (I and J). In G, solid arrow indicates a cell cluster. Hematoxylin and eosin and Masson's trichrome stained sections are shown in left and right columns, respectively. Bar indicates 0.2 mm.

Consistent with previous reports[16,27], collagen fibrils in those regions were aligned in a circular orientation, and cross-sections of collagen fibrils were observed on the sections prepared perpendicular to the meniscus surfaces. Electron microscopy of control lateral menisci revealed that collagen fibrils of various diameters were densely packed in the matrix [Fig. 6(A)]. In OA lateral menisci, the change of collagen fibrils was rather modest, though fibrils of thinner diameters could have increased in

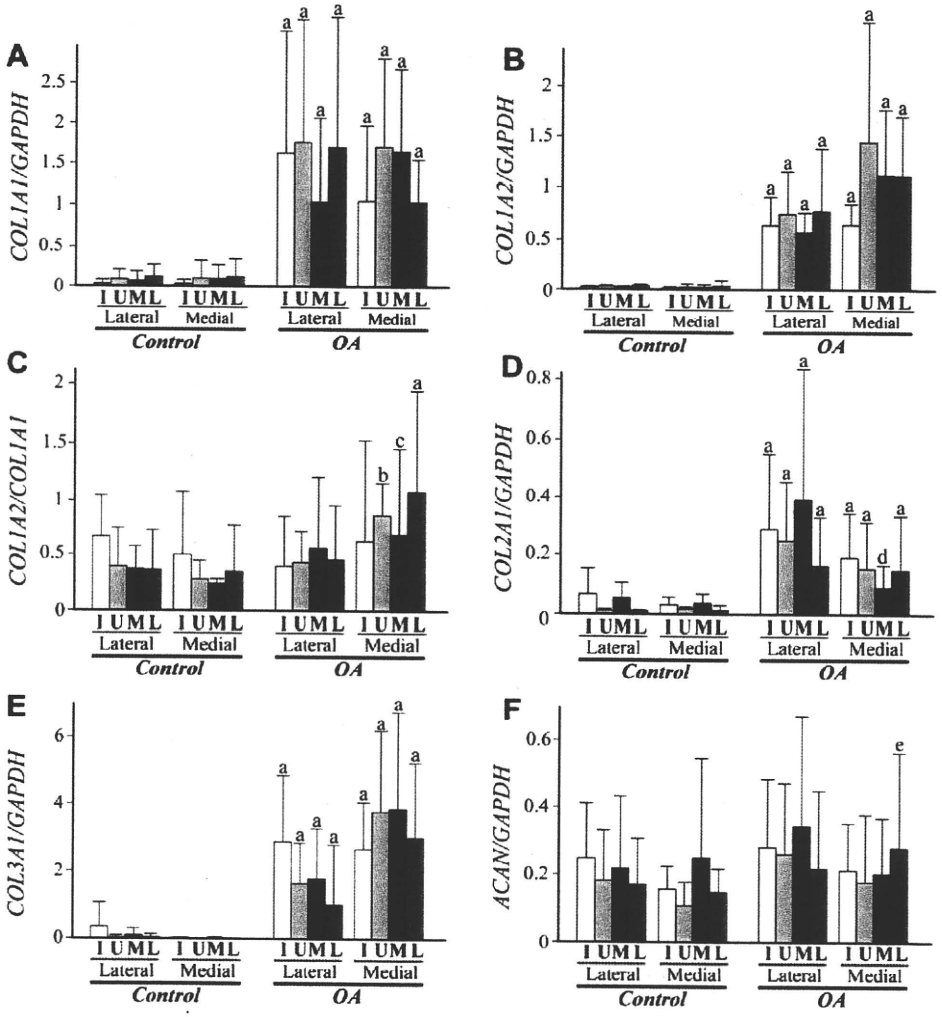

Fig. 4. Expression of matrix genes in OA and control menisci. Anterior horn segment of a meniscus was divided into four regions, and expression of matrix genes was evaluated in respective regions. Expression of type I (A and B), type II (D), type III (E) procollagen genes and aggrecan (F) is shown together with the expression ratio between two type I procollagen genes (C). In A, B, and D–F, results are shown by ratios against *GAPDH* expression. I, U, M, and L under bars indicate inner, upper surface, middle, and lower surface regions, respectively. Lateral and Medial indicate lateral and medial menisci, respectively. Results are shown by mean + 95% confidence interval. a, b, c, d and e indicate *P* values of <0.0001, 0.0092, 0.0021, 0.0086 and 0.0456, respectively, against corresponding region in control menisci.

number [Fig. 6(B)]. The change by OA was more obvious in medial menisci. Electron microscopy of the control medial menisci showed densely packed collagen fibrils with various diameters [Fig. 6(C)]. Although they resembled those of control lateral menisci, the fibrils tended to be more densely aligned. In OA medial menisci, the number of thinner fibrils increased obviously, and the fibrils were placed more sparsely [Fig. 6(D)]. The result of quantitative image analysis revealed that in OA medial menisci, the mean fibril diameter and percentage of the area occupied by fibrils were both significantly reduced, and the number of fibrils per area was significantly increased [Fig. 6(E)–(G)]. In lateral menisci, none of these parameters changed significantly by OA.

Biomechanical evaluation

Finally, the change in mechanical properties of meniscal matrix was evaluated by confined compression testing. Comparison of creep curves indicated that the mechanical properties could have changed by OA in medial menisci, while such changes might not be obvious in lateral menisci [Fig. 7(A)]. This was delineated by the changes in biomechanical parameters. Aggregate modulus of OA medial menisci was 40% lower than that of control medial menisci, whereas it differed little in lateral menisci [Fig. 7(B)]. In medial menisci, permeability changed more obviously. The permeability of OA medial menisci was more than 4-fold greater than that of the control medial menisci, while it changed little in lateral menisci [Fig. 7(C)]. Compared with these two parameters, the change of water content was modest. Although it tended to be higher in OA medial menisci, the increase was below the level of significance, and no significant change in this parameter was found between any two menisci [Fig. 7(D)].

Discussion

In this study, all OA menisci were obtained from OA knees with medial involvement, and the medial menisci were severely degenerated in the body segments. However, even in those menisci, the anterior horn segments were preserved well. This is why we performed most evaluations on the anterior horn segments, which made it possible to compare OA and control menisci in a site-to-site manner.

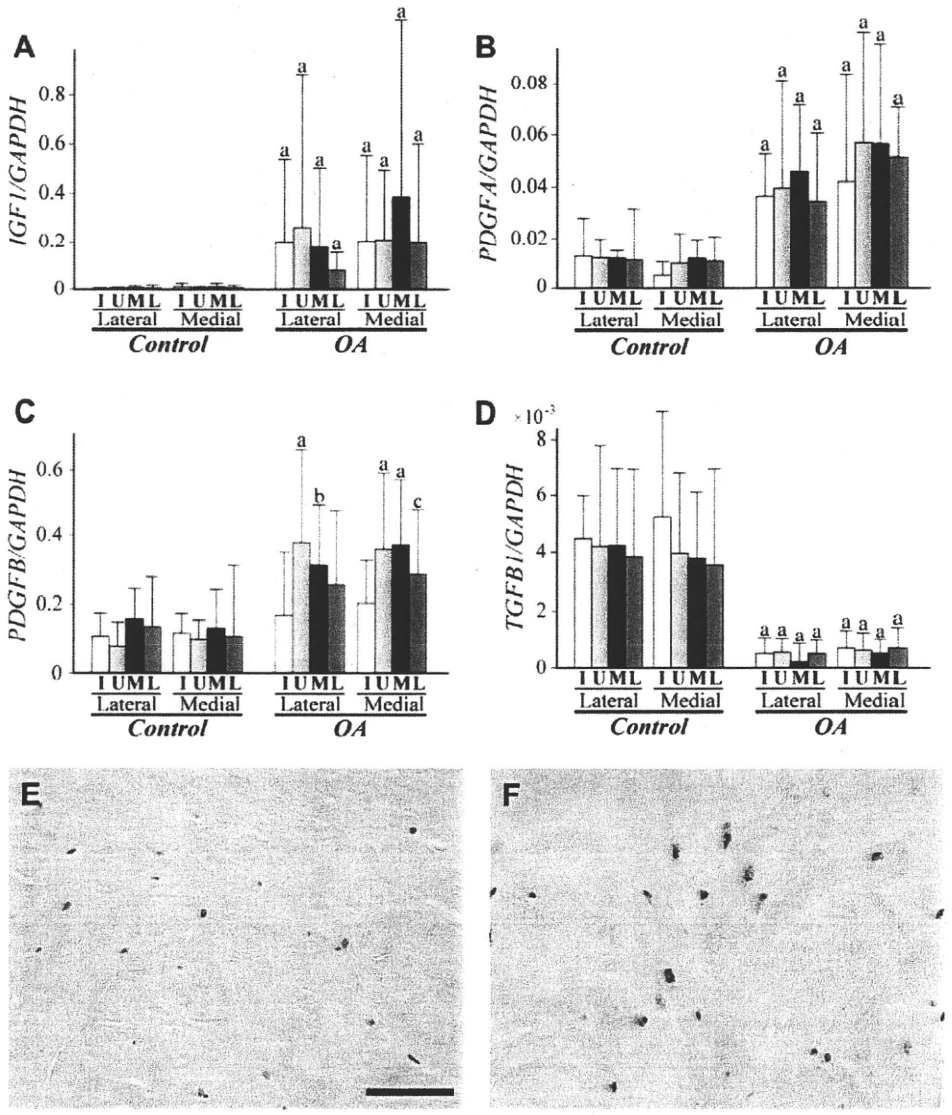

Fig. 5. Expression of possible anabolic factors in OA and control menisci. (A–D) Expression of *IGF1* (A), *PDGFA* (B), *PDGFB* (C) and *TGFB1* (D) in respective regions of OA and control menisci. Results are shown in the manner described for Fig. 4. a, b and c indicate *P* values of <0.0001, 0.0106 and 0.0028, respectively, against corresponding region in control menisci. (E and F) Immunohistochemistry for IGF-1. Photomicrographs of the sections from the middle regions of control (E) and OA menisci (F) are shown. Nuclei were stained with hematoxylin. Bar indicates 10 μm.

Consistent with the macroscopic appearance, the change in histology was moderate in the anterior horn segments of OA menisci. However, despite this limited change in histology, mRNA expression of major matrix components was markedly enhanced there. Among the five genes investigated, the increase in expression was most obvious with type I and type III procollagen, followed by type II procollagen, and least with aggrecan. This change in matrix gene expression could be the result of a reparative response that occurred within OA menisci. During the healing of fibrous tissues such as a ligament, tendon or skin, fibroblasts express type I and type III procollagens abundantly with the preponderance of type III procollagen[28,29]. We assume that this same mechanism could be involved in the enhancement of matrix gene expression in OA menisci. The result that the expression of type III procollagen tended to be more enhanced in the medial OA menisci than the lateral ones might suggest that such a reparative response could be more obvious in the medial compartment. This understanding seems reasonable since all OA knees studied here were medially involved in the disease.

Table II
[^{3}H]proline incorporation into meniscal explants

Meniscus		Scintillation count (cpm/μg DNA) (95% confidence interval)
Control	Lateral	3213 (0, 6963)
	Medial	3813 (1919, 5707)
OA	Lateral	7004 (0, 16,402)
	Medial	8345 (0, 20,875)

The result of qPCR analysis also revealed that the expression of IGF-1 was increased in OA menisci. Since IGF-1 has potent anabolic actions on meniscal cells[30–32], we consider that the increase in IGF-1 expression could be responsible for the enhanced matrix gene expression in OA menisci. In contrast to IGF-1, the expression of TGF-β1 was found to be reduced in OA menisci. This reduction in TGF-β1 expression could have a significant contribution to the degeneration of meniscal matrix. Besides the anabolic actions, TGF-β1

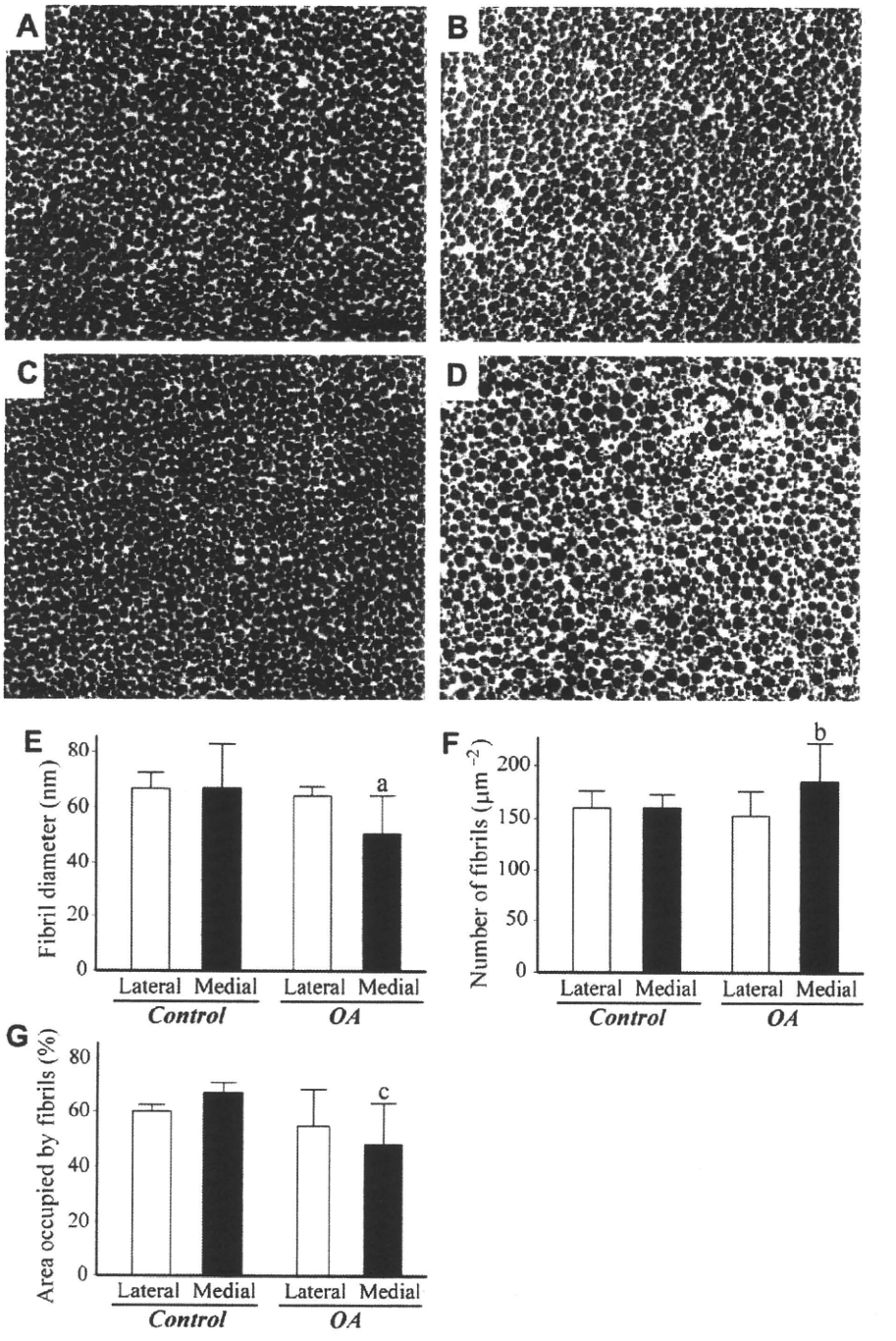

Fig. 6. Result of transmission electron microscopy. (A–D) Cross-sectional images of collagen fibrils. Electron microscopy was performed on tissues from the middle regions of control (A) and OA lateral menisci (B), and control (C) and OA medial menisci (D). Bar indicates 500 nm. (E–G) Results of quantitative image analysis. Collagen fibril diameter (E), number of fibrils per μm^2 (F), and percentage of the area occupied by fibrils (G) are shown. Lateral and Medial denote lateral and medial menisci, respectively. Results are shown by mean + 95% confidence interval. a, b and c indicate *P* values of 0.0027, 0.0423 and 0.0128, respectively, against control medial menisci.

also has a capacity to counteract the catabolic actions of proinflammatory cytokines on meniscal cells[33]. In fibroblasts and chondrocytes, TGF-β1 is known to suppress the expression of various proteinases that promote matrix degeneration, while enhancing the expression of endogenous inhibitors for those proteinases[34–37]. Therefore, the reduction of TGF-β1 expression could make the menisci more susceptible for degeneration. We assume that this might be one of the mechanisms for the loss of meniscal matrix in OA.

Interestingly, in human OA menisci, the high level of procollagen gene expression was not accompanied by a proportional increase in protein synthesis. Compared with the dramatic increase in procollagen gene expression, the increase of [^{3}H]proline incorporation was only modest. Although this seemed contradictory, the results of histological, ultrastructural, and biomechanical evaluations consistently indicated limited change of matrix in OA menisci. The reason(s) for this discrepancy is currently not known. Collagen synthesis is a complex process involving at least nine distinctive

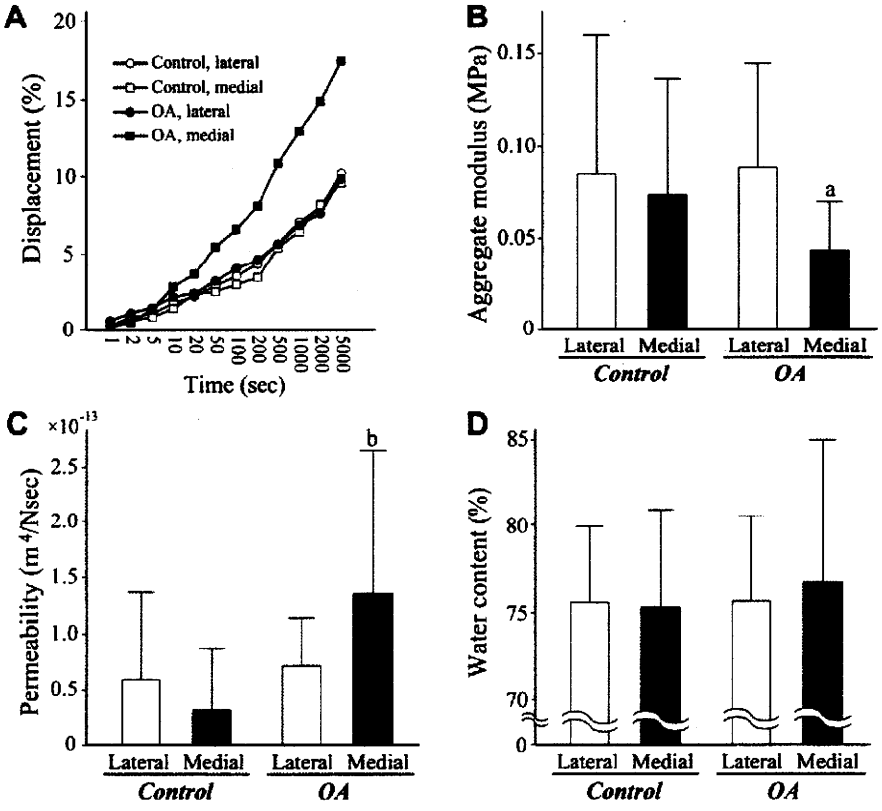

Fig. 7. Result of biomechanical measurement. Creep curve (A), aggregate modulus (B) and permeability (C) of OA and control menisci are shown together with the water content (D). In A, gray and black lines indicate the results of control and OA menisci, respectively, where circles and squares, either open or closed, denote those of lateral and medial menisci, respectively. Results are shown by mean (A) or mean + 95% confidence interval (B–D). a and b indicate *P* values of 0.0096 and <0.0001, respectively, against control medial menisci.

steps, each requiring a specific set of enzymes and chaperons[38,39]. Even after secretion, collagen molecules need to be properly processed and cross-linked outside the cells, which require another set of enzymes[40–42]. Considering these complexities, the synthetic process may well be significantly impaired at a certain step(s) in OA menisci. Future studies will clarify at which step(s), in fact, the process is impaired.

Although the change of menisci in OA has not been known well in human, several researchers have investigated it in animals. In an OA model in rabbits, cell density in the menisci was either increased or decreased depending on the regions, and cell clusters were frequently found in the degenerated areas[5,27]. However, these changes were not apparent in human OA menisci. Meanwhile, enhanced matrix gene expression was observed for both human and animal OA menisci[6,43], though the enhancement might be more intense and more comprehensive in humans.

Results of histological and molecular biological analyses revealed another difference between human and animal menisci. In animals, structural and functional heterogeneity within menisci has been reported repeatedly by many investigators: the inner areas are more like hyaline cartilage, while the outer areas have characteristics of fibrocartilage[8–11,17–19]. Differences between surface and central regions have been reported[4,17], and these were our rationale to evaluate gene expression in respective regions of menisci. However, such regional differences were not obvious in human menisci. Also, although reported with rabbit menisci[44], the difference in cell metabolism between medial and lateral menisci was not observed in human. These discrepancies between human and animal menisci should be kept in mind when meniscus pathology is studied in animal experiments.

The results of ultrastructural and biomechanical evaluations delineated the difference of matrix between lateral and medial OA menisci. This difference could be partly ascribed to the difference in type III procollagen expression. During fibril formation, type III procollagen is known to bind to type I collagen molecules and inhibit their lateral assembly[45]. The expression of type III procollagen was more promoted in OA medial menisci, and we assume that it could account for the appearance of thin collagen fibrils in those menisci. Of course, the change of meniscal matrix is not so simple, and other factors are likely involved in the process. For example, given that all OA medial menisci were severely degenerated in the body segment, the loss of structural integrity could be related to the change. Again, since catabolism is more promoted in the involved side of the knee, it might explain the change of matrix in the medial menisci. During the long course of disease progression, these factors could have worked together to alter the matrix in medial menisci.

Although we have identified several unique features of the changes in menisci with OA, this study has several limitations as well. First, since all menisci were obtained from aged donors, the results could be biased by age-related changes. We assume that this might explain, at least partly, the observed difference between human and animal menisci. If menisci from younger donors have been analyzed, that difference might not be so obvious as we observed in this study. Second, in this work, the analyses were performed mostly on the anterior horn segments of menisci, and the changes in the other parts of menisci were not investigated.

Thus, the difference among the three segments of menisci is not known, nor are the changes in the degenerated regions of OA menisci. Third, the analyses on OA menisci were done only on those from end-stage OA knees, and the menisci from early stage OA knees were not investigated. Fourth, although the involvement of IGF-1 has been suggested, the entire mechanism(s) for enhanced matrix gene expression in OA menisci has not been determined. Lastly, as stated earlier, the mechanism(s) for dissociation between enhanced matrix gene expression and modest increase in collagen synthesis has not been identified. Those points should be clarified by future studies.

As mentioned before, menisci are essential components of a knee joint. Clinically, it is well recognized that meniscus pathology is closely linked to the development and progression of knee OA[14,15,46]. Therefore, to understand the pathology of knee OA, it is essential to dissect the change of menisci in OA. Although many questions are left unanswered, we believe that the results of this study would provide some novel information on this issue.

Author contributions

Katsuragawa and Fukui had full access to all of the data in the study and take responsibility for the integrity of the data and the accuracy of the data analyses.

Conception and design. Katsuragawa and Fukui.

Analysis and interpretation of data. Katsuragawa, Furukawa, Yagishita, Mitomi and Fukui.

Drafting of the article. Katsuragawa and Fukui.

Critical revision of the article. Suzuki and Tohma.

Provision of study materials. Katsuragawa and Sawabe.

Technical support. Saitoh, Tanaka, Wake, Ikeda and Ishiyama.

Conflict of interest

The authors have no conflict of interest to disclose with regard to the subject matter of this present manuscript.

Acknowledgments

This study was supported by a Grant-in-Aid from the Japan Foundation for the Promotion of International Medical Research Cooperation to YK, and Grants-in-Aid from the Japan Society for the Promotion of Science (Grants 15390467 and 18390424) to NF.

References

1. Guccione AA, Felson DT, Anderson JJ, Anthony JM, Zhang Y, Wilson PW, *et al.* The effects of specific medical conditions on the functional limitations of elders in the Framingham Study. Am J Public Health 1994;84:351–8.
2. Noble J, Hamblen DL. The pathology of the degenerate meniscus lesion. J Bone Joint Surg Br 1975;57:180–6.
3. Cheung HS. Distribution of type I, II, III and V in the pepsin solubilized collagens in bovine menisci. Connect Tissue Res 1987;16:343–56.
4. Eyre DR, Wu JJ. Collagen of fibrocartilage: a distinctive molecular phenotype in bovine meniscus. FEBS Lett 1983;158: 265–70.
5. Hellio Le Graverand MP, Vignon E, Otterness IG, Hart DA. Early changes in lapine menisci during osteoarthritis development: Part I: cellular and matrix alterations. Osteoarthritis Cartilage 2001;9:56–64.
6. Hellio Le Graverand MP, Vignon E, Otterness IG, Hart DA. Early changes in lapine menisci during osteoarthritis development: Part II: molecular alterations. Osteoarthritis Cartilage 2001;9: 65–72.
7. Herwig J, Egner E, Buddecke E. Chemical changes of human knee joint menisci in various stages of degeneration. Ann Rheum Dis 1984;43:635–40.
8. Kambic HE, McDevitt CA. Spatial organization of types I and II collagen in the canine meniscus. J Orthop Res 2005;23:142–9.
9. Nakano T, Dodd CM, Scott PG. Glycosaminoglycans and proteoglycans from different zones of the porcine knee meniscus. J Orthop Res 1997;15:213–20.
10. Scott PG, Nakano T, Dodd CM. Isolation and characterization of small proteoglycans from different zones of the porcine knee meniscus. Biochim Biophys Acta 1997;1336:254–62.
11. Valiyaveettil M, Mort JS, McDevitt CA. The concentration, gene expression, and spatial distribution of aggrecan in canine articular cartilage, meniscus, and anterior and posterior cruciate ligaments: a new molecular distinction between hyaline cartilage and fibrocartilage in the knee joint. Connect Tissue Res 2005;46:83–91.
12. Wojtys EM, Chan DB. Meniscus structure and function. Instr Course Lect 2005;54:323–30.
13. Gale DR, Chaisson CE, Totterman SM, Schwartz RK, Gale ME, Felson D. Meniscal subluxation: association with osteoarthritis and joint space narrowing. Osteoarthritis Cartilage 1999;7: 526–32.
14. Berthiaume MJ, Raynauld JP, Martel-Pelletier J, Labonte F, Beaudoin G, Bloch DA, *et al.* Meniscal tear and extrusion are strongly associated with progression of symptomatic knee osteoarthritis as assessed by quantitative magnetic resonance imaging. Ann Rheum Dis 2005;64:556–63.
15. Hunter DJ, Zhang YQ, Niu JB, Tu X, Amin S, Clancy M, *et al.* The association of meniscal pathologic changes with cartilage loss in symptomatic knee osteoarthritis. Arthritis Rheum 2006;54: 795–801.
16. Petersen W, Tillmann B. Collagenous fibril texture of the human knee joint menisci. Anat Embryol (Berl) 1998;197: 317–24.
17. Kavanagh E, Ashhurst DE. Distribution of biglycan and decorin in collateral and cruciate ligaments and menisci of the rabbit knee joint. J Histochem Cytochem 2001;49:877–85.
18. Spindler KP, Miller RR, Andrish JT, McDevitt CA. Comparison of collagen synthesis in the peripheral and central region of the canine meniscus. Clin Orthop Relat Res 1994;256–63.
19. Upton ML, Hennerbichler A, Fermor B, Guilak F, Weinberg JB, Setton LA. Biaxial strain effects on cells from the inner and outer regions of the meniscus. Connect Tissue Res 2006;47: 207–14.
20. Altman R, Asch E, Bloch D, Bole G, Borenstein D, Brandt K, *et al.* Development of criteria for the classification and reporting of osteoarthritis. Classification of osteoarthritis of the knee. Diagnostic and Therapeutic Criteria Committee of the American Rheumatism Association. Arthritis Rheum 1986; 29:1039–49.
21. Fukui N, Miyamoto Y, Nakajima M, Ikeda Y, Hikita A, Furukawa H, *et al.* Zonal gene expression of chondrocytes in osteoarthritic cartilage. Arthritis Rheum 2008;58:3843–53.
22. Tashiro T, Hiraoka H, Ikeda Y, Ohnuki T, Suzuki R, Ochi T, *et al.* Effect of GDF-5 on ligament healing. J Orthop Res 2006;24:71–9.
23. Joshi MD, Suh JK, Marui T, Woo SL. Interspecies variation of compressive biomechanical properties of the meniscus. J Biomed Mater Res 1995;29:823–8.
24. Mow VC, Kuei SC, Lai WM, Armstrong CG. Biphasic creep and stress relaxation of articular cartilage in compression? Theory and experiments. J Biomech Eng 1980;102:73–84.
25. Ingman AM, Ghosh P, Taylor TK. Variation of collagenous and non-collagenous proteins of human knee joint menisci with age and degeneration. Gerontologia 1974;20:212–23.

26. Ghosh P, Ingman AM, Taylor TK. Variations in collagen, non-collagenous proteins, and hexosamine in menisci derived from osteoarthritic and rheumatoid arthritic knee joints. J Rheumatol 1975;2:100–7.
27. Bullough PG, Munuera L, Murphy J, Weinstein AM. The strength of the menisci of the knee as it relates to their fine structure. J Bone Joint Surg Br 1970;52:564–7.
28. Liu SH, Yang RS, al-Shaikh R, Lane JM. Collagen in tendon, ligament, and bone healing. A current review. Clin Orthop Relat Res 1995;265–78.
29. Bullard KM, Longaker MT, Lorenz HP. Fetal wound healing: current biology. World J Surg 2003;27:54–61.
30. Pangborn CA, Athanasiou KA. Growth factors and fibrochondrocytes in scaffolds. J Orthop Res 2005;23:1184–90.
31. Tumia NS, Johnstone AJ. Regional regenerative potential of meniscal cartilage exposed to recombinant insulin-like growth factor-I in vitro. J Bone Joint Surg Br 2004;86:1077–81.
32. Imler SM, Doshi AN, Levenston ME. Combined effects of growth factors and static mechanical compression on meniscus explant biosynthesis. Osteoarthritis Cartilage 2004;12:736–44.
33. McNulty AL, Guilak F. Integrative repair of the meniscus: lessons from in vitro studies. Biorheology 2008;45:487–500.
34. Gunther M, Haubeck HD, van de Leur E, Blaser J, Bender S, Gutgemann I, *et al.* Transforming growth factor beta 1 regulates tissue inhibitor of metalloproteinases-1 expression in differentiated human articular chondrocytes. Arthritis Rheum 1994;37:395–405.
35. Qureshi HY, Sylvester J, El Mabrouk M, Zafarullah M. TGF-beta-induced expression of tissue inhibitor of metalloproteinases-3 gene in chondrocytes is mediated by extracellular signal-regulated kinase pathway and Sp1 transcription factor. J Cell Physiol 2005;203:345–52.
36. Edwards DR, Murphy G, Reynolds JJ, Whitham SE, Docherty AJ, Angel P, *et al.* Transforming growth factor beta modulates the expression of collagenase and metalloproteinase inhibitor. EMBO J 1987;6:1899–904.
37. Overall CM, Wrana JL, Sodek J. Independent regulation of collagenase, 72-kDa progelatinase, and metalloendoproteinase inhibitor expression in human fibroblasts by transforming growth factor-beta. J Biol Chem 1989;264:1860–9.
38. Canty EG, Kadler KE. Procollagen trafficking, processing and fibrillogenesis. J Cell Sci 2005;118:1341–53.
39. Lamande SR, Bateman JF. Procollagen folding and assembly: the role of endoplasmic reticulum enzymes and molecular chaperones. Semin Cell Dev Biol 1999;10:455–64.
40. Prockop DJ, Sieron AL, Li SW. Procollagen N-proteinase and procollagen C-proteinase. Two unusual metalloproteinases that are essential for procollagen processing probably have important roles in development and cell signaling. Matrix Biol 1998;16:399–408.
41. Myllyharju J, Kivirikko KI. Collagens and collagen-related diseases. Ann Med 2001;33:7–21.
42. Kagan HM, Li W. Lysyl oxidase: properties, specificity, and biological roles inside and outside of the cell. J Cell Biochem 2003;88:660–72.
43. Wildey GM, Billetz AC, Matyas JR, Adams ME, McDevitt CA. Absolute concentrations of mRNA for type I and type VI collagen in the canine meniscus in normal and ACL-deficient knee joints obtained by RNase protection assay. J Orthop Res 2001;19:650–8.
44. Hellio Le Graverand MP, Reno C, Hart DA. Gene expression in menisci from the knees of skeletally immature and mature female rabbits. J Orthop Res 1999;17:738–44.
45. Romanic AM, Adachi E, Kadler KE, Hojima Y, Prockop DJ. Copolymerization of pNcollagen III and collagen I. pNcollagen III decreases the rate of incorporation of collagen I into fibrils, the amount of collagen I incorporated, and the diameter of the fibrils formed. J Biol Chem 1991;266:12703–9.
46. Englund M, Roos EM, Lohmander LS. Impact of type of meniscal tear on radiographic and symptomatic knee osteoarthritis: a sixteen-year followup of meniscectomy with matched controls. Arthritis Rheum 2003;48:2178–87.

Knee Surg Sports Traumatol Arthrosc (2011) 19:424–431
DOI 10.1007/s00167-010-1246-6

KNEE

Anatomical placement of double femoral tunnels in anterior cruciate ligament reconstruction: anteromedial tunnel first or posterolateral tunnel first?

Shuji Taketomi · Takumi Nakagawa · Hideki Takeda · Kohei Nakajima · Shuichi Nakayama · Atsushi Fukai · Jinso Hirota · Yoshinori Kachi · Hirotaka Kawano · Toshiki Miura · Naoshi Fukui · Kozo Nakamura

Received: 19 April 2010 / Accepted: 9 August 2010 / Published online: 3 September 2010

Abstract
Purpose The purpose of this study was to know which tunnel—the anteromedial (AM) bundle or the posterolateral (PL) bundle—should be prepared first to create the 2 femoral tunnels accurately in anatomic double-bundle (DB) anterior cruciate ligament (ACL) reconstruction.
Methods Thirty-four patients were divided into 2 groups of 17 depending on the sequence of preparation of the 2 femoral tunnels. In group A, the AM tunnel was prepared first, whereas the PL tunnel was prepared first in group P. ACL reconstruction was performed using a three-dimensional (3-D) fluoroscopy-based navigation system to place the double femoral tunnels through an accessory medial portal. The double femoral socket positioning was evaluated by 3-D computed tomography (CT) scan image.
Results The non-anatomical placement of the femoral sockets occurred in 5 patients (29%) in group A, whereas the 2 sockets were placed anatomically in all patients in group P ($P < 0.05$). Evaluation of the AM and the PL socket location on the 3-D CT images using the quadrant method showed more similar values to the laboratory data in a literature in group P than in group A. No complication occurred in group A, whereas complications such as socket communications or back wall blowout occurred in 5 patients (29%) in group P ($P < 0.05$).
Conclusion The sequence of creating 2 femoral tunnels through accessory medial portal affected the resultant location of the sockets and the rate of the complications. When femoral tunnels are prepared with a transportal technique, PL tunnel first technique seems to be superior to AM first technique regarding anatomic placement. However, PL tunnel first technique accompanies the risk of socket communication.

Keywords Anterior Cruciate Ligament (ACL) · Double-bundle ACL reconstruction · Navigation · Femoral tunnel · Three-dimensional CT

Introduction

Conventional single-bundle (SB) anterior cruciate ligament (ACL) reconstruction has demonstrated good clinical results [23]; however, patients with reconstructed knees occasionally develop a degenerative change including medial meniscus injury and osteoarthritis [15]. Recently, better knowledge of ACL anatomy and function has led to "anatomic" ACL reconstruction [4, 6, 8, 10, 25]. Anatomic double-bundle (DB) ACL reconstruction, reproducing anteromedial (AM) and posterolateral (PL) bundles within the native ACL insertion, has been introduced to offer better biomechanical outcomes, especially in controlling rotatory loads [24, 29]. Various surgical techniques for anatomic ACL reconstruction using hamstrings [21, 26, 32], bone-patellar tendon-bone [17, 18], or quadriceps tendon [14, 20] have been reported. One of the most important factors influencing the surgical outcome after ACL reconstruction might be the placement of the femoral socket. If the femoral sockets are not positioned within the native ACL insertion, rotatory instability and impingement on the roof or the posterior cruciate ligament might occur [5]. It is technically difficult to place the 2 femoral

S. Taketomi · T. Nakagawa (✉) · H. Takeda · K. Nakajima · S. Nakayama · A. Fukai · J. Hirota · Y. Kachi · H. Kawano · T. Miura · N. Fukui · K. Nakamura
Department of Orthopaedic Surgery, Faculty of Medicine, The University of Tokyo, 7-3-1 Hongo, Bunkyo-ku, Tokyo 113-0033, Japan
e-mail: takumin-tky@umin.ac.jp

sockets in ideal positions reproducibly, even for experienced surgeons.

Many techniques have been reported to create the femoral tunnels including the traditional transtibial technique [11, 27], the outside-in technique in which the femoral guide pin is placed transfemorally from the outside [13, 28], and the transportal technique using a medial portal or an accessory medial portal [3, 12, 21]. We used a three-dimensional (3-D) fluoroscopy-based navigation system to place the 2 femoral tunnels accurately and reproducibly through an accessory medial portal [16]. With respect to the transportal technique, some authors prepared the AM tunnel first [12], whereas others prepared the PL tunnel first [30]; however, there has been no definite recommendation regarding which tunnel should be prepared first [30]. Therefore, the purpose of this study was to learn which one should be prepared first to create the 2 femoral tunnels, accurately in anatomic DB ACL reconstruction. We hypothesized that the sequence of preparing 2 femoral tunnels (AM first technique or PL first technique) would affect the accuracy and consistency of socket positioning in anatomic DB ACL reconstruction. Consecutive ACL reconstruction cases were divided into 2 groups depending on the sequence of preparing the femoral tunnels, i.e., AM first group or PL first group. We evaluated the position of the femoral sockets after anatomic DB ACL reconstruction using 3-D computed tomography (CT) scan images that were performed a week after surgery.

Materials and methods

Of the 37 consecutive patients on whom the ACL reconstruction was performed in our institute between July 2008 and August 2009, 34 met the inclusion criteria. In this study, these criteria were as follows: (1) using a 3-D fluoroscopy-based navigation system for operation, (2) using hamstring grafts for DB ACL reconstruction, (3) no prior intra-articular or extra-articular ligament reconstruction, and (4) no history of distal femoral fracture. The patients included 13 women and 21 men with an average age of 31 years (range 15–63). They were divided into 2 groups based on the sequence of preparing the 2 femoral tunnels. In group A, the AM tunnel was prepared prior to the PL tunnel and ACL reconstruction on these patients was performed between July 2008 and April 2009. In group P, the PL tunnel was prepared first when creating the 2 femoral tunnels and surgery on these patients was carried out between May 2009 and August 2009; there were 17 patients in each group. The mean AM socket diameter was 5.6 ± 0.3 mm in group A and was 5.5 ± 0.6 mm in group P, while the mean PL socket diameter was 5.3 ± 0.4 mm in group A, and was 5.0 ± 0.2 mm in group P. There was no significant difference in the stature of the patients in these 2 groups (n.s.). The surgeries were performed by 4 knee surgeons through this period. Information about patient is summarized in Table 1. The patients and their families were informed that data from their cases would be submitted for publication, and all gave their consent.

Table 1 Patient information

	Group A	Group P	
Number of patients	17	17	
Sex (Female/male)	5/12	8/9	
Age (years)	31 ± 13 (15–63)	31 ± 11 (17–51)	
Body height (cm)	169.7 ± 7.2	168.2 ± 7.0	n.s.
Body weight (kg)	66.6 ± 8.3	63.4 ± 15.7	n.s.
Body mass index (BMI)	23.1 ± 2.0	22.2 ± 4.2	n.s.

Surgical procedure

ACL reconstruction was arthroscopically performed using a 3-D fluoroscopy-based navigation system to place the double femoral tunnels [16]. Intra-operative 3-D images were acquired with the C-arm of Arcadis Orbic 3-D (Siemens AG, Erlangen, Germany) after the reference frame was attached rigidly to the femur. The acquired image data were downloaded to the navigation computer (StealthStation TRIA plus; Medtronic), and a 3-D image of the distal femur was reconstructed on the computer screen. The medial half of the 3-D reconstructed distal femur was deleted using computer software for a better view of the lateral wall and the roof of the femoral intercondylar notch. The hamstring tendons were harvested, and the doubled grafts were looped over EndoButton CLs (Smith & Nephew Endoscopy, Andover, MA). The anatomic insertion site of each native ACL bundle was marked on the femur and tibia by a radiofrequency device. The femoral insertion site of each bundle was determined in reference to the bony landmarks (i.e. the lateral intercondylar ridge and the lateral bifurcate ridge) both arthroscopically and on the 3-D reconstructed image [8, 9]. An arthroscope was introduced through a medial portal, and the tip of the femoral guide through an accessory medial portal was placed at the center of the AM and the PL bundle's femoral footprint, respectively (Fig. 1). Keeping the femoral guide tip at the center of the AM or the PL footprint, the knee was flexed to 120° to 130°. On the navigation computer screen, the surgeon confirmed the anatomically correct placement of the tip of the femoral guide. The risk of a back wall blowout was also evaluated, and the virtual exit of the femoral tunnel on the monitor enabled us to estimate the length of the tunnel. After the guidewire for the femoral tunnel was placed, the wire was overdrilled for an adequate

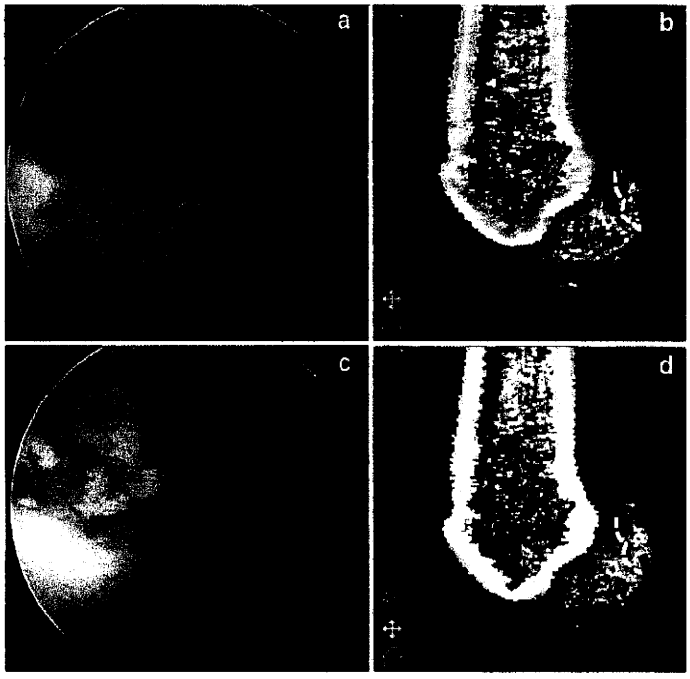

Fig. 1 **a**, **c** The tip of the femoral guide was placed at the center of the anteromedial (AM) and posterolateral (PL) bundle's femoral footprint through an accessory medial portal. **b**, **d** The lateral wall and the roof of the femoral intercondylar notch, and the lateral intercondylar ridge (*broken line*) on the three-dimensional (3-D) reconstructed image. *Arrow* shows the tip of the femoral guide placed at the center of the AM bundle and the PL bundle, respectively

length using a cannulated drill, and the lateral femoral cortex was drilled through using an EndoButton drill (Smith & Nephew Endoscopy, Andover, MA). The AM tunnel was created first in group A, while the PL tunnel was created first in group P (Fig. 1). The other surgical methods were same in both groups.

Evaluation of the position of femoral sockets with 3-D CT scan

Three-dimensional CT scan image of the operated knee was done a week after surgery. Medical research center ethics committee of our institute approved this study including the use of a postoperative CT scan. The CT machine was a helical high-speed Aquilion™ 64 or Aquilion ONE™ (Toshiba Medical Systems Co., Japan). Then, 3-D reconstruction of the operated knee was performed using the ZIOSTATION software package (Ziosoft Inc., Tokyo, Japan). The tibia, the patella, and the medial femoral condyle were removed as necessary to visualize the lateral wall of the intercondylar notch. All measurements were taken on the surface of the lateral wall of the intercondylar notch completely in an orthogonal projection to the view angle of the surface being measured to ensure accuracy. According to Basdekis et al. [1], the measurement error of this evaluating method was very small.

We determined whether the 2 femoral sockets were positioned within the femoral insertion of the native ACL on the 3-D CT scan image. In a case where the lateral intercondylar ridge could be seen on the 3-D CT scan image, we defined both the AM and the PL sockets positioned posterior to the lateral intercondylar ridge as anatomic socket placements [8] (Fig. 2). In a case where the lateral intercondylar ridge could not be clearly seen on the image, we defined the 2 femoral sockets positioned posterior to the extended line from the posterior cortex of the distal femur as anatomic socket placements, in reference to the reports by Giron et al. [10] (Fig. 3). In addition, as the complication in preparing the femoral tunnels, the communication between the AM socket and the PL socket, and the back wall blowout were elucidated by the 3-D CT scan image (Fig. 4).

Morphometric assessment of the femoral socket positioning of the AM and the PL bundles was performed according to the quadrant technique as described by Bernard and Hertel [2]. The total sagittal diameter of the lateral condyle along Blumensaat's line (D) and maximum lateral intercondylar notch height (H) were measured on the 3-D CT scan image. The distance from the center of the AM or the PL socket to the most dorsal subchondral contour of the lateral femoral condyle (d) and the distance from the center of each socket to Blumensaat's line (h) were measured (Fig. 5). The length of distance d as a partial distance of D and the height of the distance h as a partial distance of H were expressed in percentages, such as d/D and h/H%, respectively. All measurements were taken by one orthopedic surgeon and were repeated at 3-month interval. For morphometric assessment using the

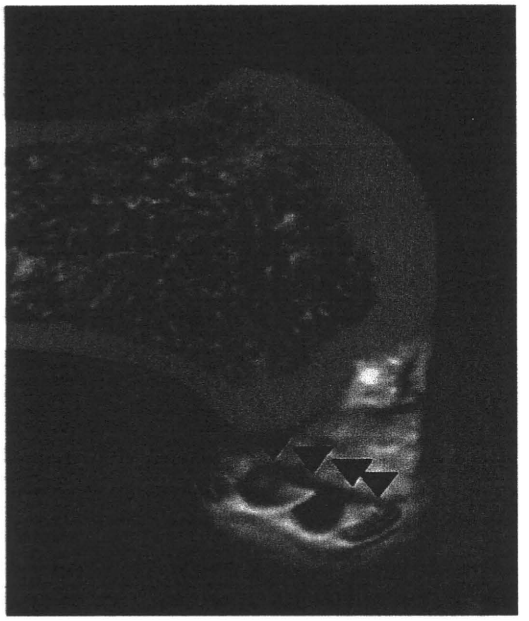

Fig. 2 The 2 femoral sockets were prepared anatomically just posterior to and below the lateral intercondylar ridge (*triangles*) with the knee in 90° of flexion on the 3-D CT scan image

quadrant technique, a mean of these repeated measurements was recorded and intra-observer variability was calculated.

Statistical analysis

Statistical analysis was done using the EXCEL statistics 2008 (SSRI Co., Ltd., Tokyo, Japan) software package for Microsoft Windows. Fisher's exact test was used to compare the rate of complication and the rate of anatomical femoral socket placement. Paired *t* test was used to compare the femoral socket positioning using the quadrant technique and the stature, body weight, and body mass index of patients. The statistical significance level was set at $P < 0.05$.

Results

The non-anatomical placement of the femoral sockets was found in 5 patients (29%) in group A on the 3-D CT scan image evaluation, whereas both sockets were placed within the native femoral insertion in all patients in group P. The rate of anatomical femoral socket positioning was significantly higher in group P than in group A ($P = 0.04$). (Table 2) No complication in preparing the femoral sockets was found in group A; however, it was found in 5 patients (29%) in group P. The socket communications occur in 4 patients, and the back wall blowout was found in 1 patient. (Table 2) The rate of complication was significantly higher in group P than in group A ($P = 0.04$).

The assessment of the femoral socket positioning on the 3-D CT scan image according to the quadrant technique described by Bernard and Hertel [2] showed that the center of the AM socket was located at d/D = 22.4 ± 4.3% and h/H = 35.3 ± 10.6% in group A, whereas it was located at d/D = 20.1 ± 4.8% and h/H = 27.3 ± 6.1% in group P, respectively. In the same way, the center of the PL socket was located at d/D = 35.0 ± 7.9% and h/H = 59.5 ± 7.5% in group A, whereas it was located at d/D = 30.2 ± 6.5% and h/H = 53.6 ± 5.8% in group P, respectively (Table 3 and Fig. 6). The values of h/H for the AM socket and the PL socket were significantly larger in group A than in group P ($P = 0.01$ and $P = 0.01$, respectively). No significant difference was found in the values of d/D for the 2 sockets between group A and group P (n.s.). The intra-observer difference was 1.3 ± 1.2%. Laboratory data described by the quadrant method [31] are shown at the bottom of the Table 3.

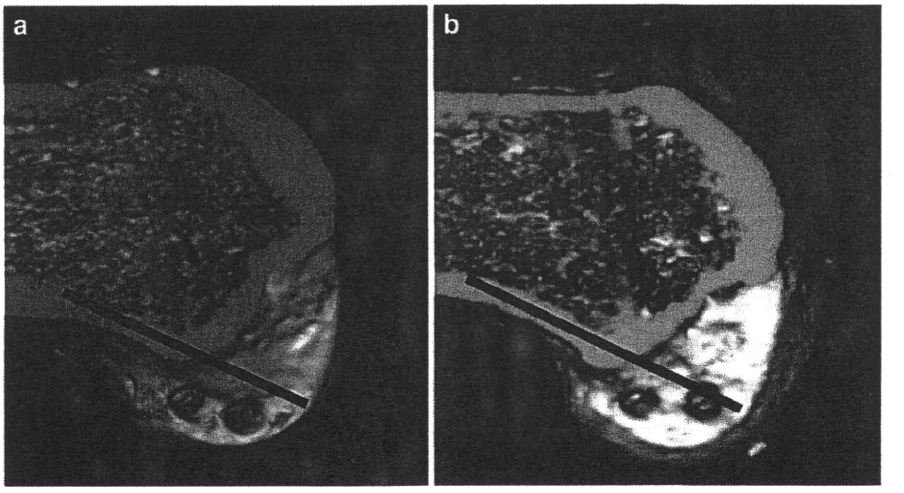

Fig. 3 When the lateral intercondylar ridge could not be seen on the 3-D CT scan image, we defined the 2 femoral sockets positioned below the extended line from the posterior cortex as being correct socket within the native anterior cruciate ligament (ACL). **a** The 2 femoral sockets within the femoral insertion of the native ACL, **b** the PL socket protruded from the femoral insertion of the native ACL

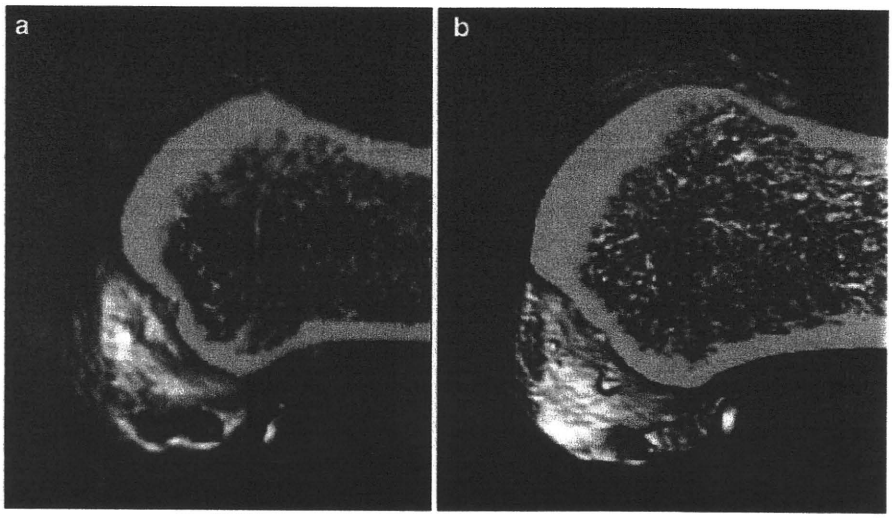

Fig. 4 **a** The communication between the AM socket and the PL socket on the 3-D CT scan image, **b** the back wall blowout of the AM tunnel on the 3-D CT scan image

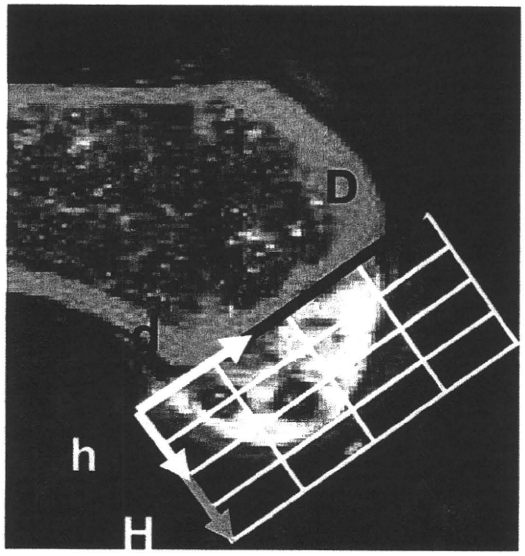

Fig. 5 Measurements of the femoral socket positioning using the quadrant method described by Bernard and Hertel [2]. The total sagittal diameter of the lateral condyle along Blumensaat's line (D) and maximum lateral intercondylar notch height (H) were measured on the 3-D CT scan image. The distance from the center of the AM or the PL socket to the most dorsal subchondral contour of the lateral femoral condyle (d) and the distance from the center of the AM or the PL socket to Blumensaat's line (h) were measured

Discussion

The most important finding of the present study was that the sequence of drilling affected the position of the femoral sockets. When the AM tunnel was prepared prior to the PL tunnel preparation, the PL sockets were significantly apt to be positioned anterior (arthroscopically shallow) to the lateral intercondylar ridge with the knee in 90° of flexion. This shallow positioning of the PL socket might result from the intention to preserve a bony bridge and avoid socket communication with the pre-existing AM socket in group A. On the other hand, when the PL socket was prepared anatomically just posterior to the lateral intercondylar ridge with the knee in 90° of flexion, the 2 femoral sockets were positioned within the native ACL femoral insertion in all cases. However, the complications in preparing the femoral sockets occurred in 29% of the patients, which was statistically significant different from group A. It seemed that space for the AM socket was very limited in some patients because of the existence of the anatomically placed PL socket. As a result, the bony bridge could not be preserved in some cases, although the AM socket has been placed as arthroscopically deep as possible with the assistance of 3-D fluoroscopic navigation to avoid a back wall blowout.

Table 2 Rate of the anatomical femoral socket placement, the socket communication, and the back wall blowout on the three-dimensional computed tomography (3-D CT) scan image

	Anatomic socket placement	Complications	
		Socket communication	Back wall blowout
Group A ($n = 17$)	12 (71%)*	0 (0%)**	
		0 (0%)	0 (0%)
Group P ($n = 17$)	17 (100%)*	5 (29%)**	
		4 (24%)	1 (6%)

* $P = 0.04$

** $P = 0.04$

Table 3 Center of the AM bundle and the PL bundle location on the 3-D CT scan image

	Anteromedial bundle		Posterolateral bundle	
	d/D (%)	h/H (%)	d/D (%)	h/H (%)
Group A	22.4 ± 4.3	35.3 ± 10.6*	35.0 ± 7.9	59.5 ± 7.5**
Group P	20.1 ± 4.8	27.3 ± 6.1*	30.2 ± 6.5	53.6 ± 5.8**
	n.s.	*$P = 0.01$	n.s.	**$P = 0.01$
Laboratory study [31]	*18.5*	*22.3*	*29.3*	*53.6*

Center of the AM bundle and the PL bundle location on the femoral side using the quadrant method in 20 human cadaveric knees by Zantop et al. [31] is shown at the bottom of the table. The laboratory data are given in italics

d/D (%) = depth of Blumensaat's line, h/H (%) = height of the lateral femoral condyle

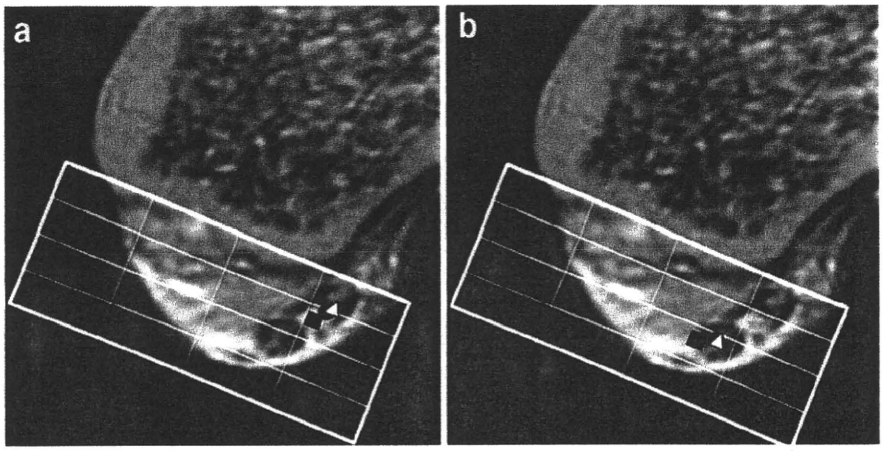

Fig. 6 Center of the AM (**a**) socket and the PL (**b**) socket location on the lateral wall of femoral notch was calculated using the quadrant method. *Square dot* showed the center of each socket in group A, *round dot* showed that in group P, and *triangular dot* showed the center of each bundle from the cadaveric data measured by Zantop et al. [31]

Colombet et al. suggested that with a 5-mm-diameter graft for the PL bundle and a 7-mm-diameter AM graft, it would be theoretically possible to place the centers of both grafts in their respective native attachment site positions, while leaving a 2-mm bony bridge between sockets [4]. Van Eck et al. recommended SB reconstruction to avoid a complication, if the femoral insertion site was less than 14 mm in diameter, in their recent literature [22]. According to Siebold et al. [19], the length of the femoral insertion varied between 10 and 19 mm, with a mean of 14 to 15 mm. Recognizing that there is an individual difference in the footprint sizes and that the figures of Japanese people are smaller than those of Europeans, there most likely would be cases in which no bony bridge can be preserved when both AM and PL sockets are placed within a narrow ACL femoral insertion.

The morphometric analysis of the femoral socket placements between group A and group P was done using the quadrant method described by Bernard and Hertel [2]. The values of h/H for the AM socket and the PL socket were significantly larger in group A than in group P. The values of d/D for the 2 sockets were larger in group A than in group P, even though no significant difference was found. Based on these calculated data, the 2 femoral sockets were positioned more posterior (arthroscopically deep) in group P than in group A. Zantop et al. reported the radiographic center of the AM and the PL attachment on the femoral side using the quadrant method in 20 human cadaveric knees [31]. According to them, the center of the AM bundle on the femoral side was 18.5 and 22.3%, whereas the center of the PL bundle on the femoral side was 29.3 and 53.6% of the depth of Blumensaat's line and the height of the femoral condyle, respectively (Table 3 and Fig. 6). These data were very similar to our calculated value using the postoperative 3-D CT image in both groups. When the mean value was compared between group A and group P, the mean value in group P was more similar to the cadaveric data than in group A.

There is also possibility that the narrow femoral notch would make creating the two anatomical sockets difficult. Between the two groups in this study, the body height of the patients, which is reported to be most significant factor affecting ACL volume [7], was not different. Therefore, the difference of the femoral notch size seemed not to be a confounding factor to affect the results of this study. Overall, our results indicate that the femoral socket placements were more anatomic in group P than in group A, although rate of the complications was high. To achieve both the anatomic socket placement while avoiding socket communication, a navigation software to calculate and

determine the appropriate position of the double femoral sockets on 3-D navigation monitor might be helpful in future. The arthroscopic caliper to measure accurately the length of lateral wall of femoral notch might be also useful.

There were some limitations to this study. The first was that the patients were not assigned into 2 groups randomly. Surgery was performed on the patients in group A at an earlier period than those in group P. The learning curve might have affected the results of the study. In other words, there is a possibility that an improvement in surgical techniques might have decreased the rate of the non-anatomical socket placement in group P. Another limitation is that the 3-D CT scan was not taken on the contralateral knee being used as control. It is difficult to evaluate the 3-D CT scan image of the operated knee alone, because the natural morphology of the lateral wall of the intercondylar notch was destroyed by the reconstructive surgery. The lateral intercondylar ridge could not be identified, and accurate evaluation of the femoral insertion was impossible in some patients. Finally, the navigation system that was used as guidance to determine the position of the femoral tunnels was a confounding factor. Therefore, there is possibility that the results of this study could not be directly applied to DB ACL reconstruction without the navigation system.

In our retrospective observation of the socket location between the two techniques, i.e. AM first technique and PL first technique, there was difference in the resultant femoral socket locations between the two techniques. Further randomized prospective studies are required in future to answer which technique—the AM first technique or the PL first technique—would be more appropriate to prepare two anatomical femoral sockets in ACL reconstruction.

Conclusion

The results of this study revealed that the sequence of drilling affected the position of the femoral sockets. Preparing the PL tunnel prior to the AM tunnel enabled us to make the double sockets consistent inside the femoral insertion of native ACL. On the other hand, the rate of complications such as socket communication or back wall blowout was significantly higher in PL tunnel first technique. We believe that it is necessary to take into account the sequence of preparing the two femoral tunnels in DB ACL reconstruction.

References

1. Basdekis G, Christel P, Anne F (2009) Validation of the position of the femoral tunnels in anatomic double-bundle ACL reconstruction with 3-D CT scan. Knee Surg Sports Traumatol Arthrosc 17:1089–1094
2. Bernard M, Hertel P, Hornung H, Cierpinski T (1997) Femoral insertion of the ACL. Radiographic quadrant method. Am J Knee Surg 10:14–22
3. Christel P, Sahasrabudhe A, Basdekis G (2008) Anatomic double-bundle anterior cruciate ligament reconstruction with anatomic aimers. Arthroscopy 24:1146–1151
4. Colombet P, Robinson J, Christel P, Franceschi J, Djian P, Bellier G, Sbihi A (2006) Morphology of anterior cruciate ligament attachments for anatomic reconstruction: a cadaveric dissection and radiographic study. Arthroscopy 22:984–992
5. Colvin A, Shen W, Musahl V, Fu F (2009) Avoiding pitfalls in anatomic ACL reconstruction. Knee Surg Sports Traumatol Arthrosc 17:956–963
6. Farrow L, Chen M, Cooperman D, Victoroff B, Goodfellow D (2007) Morphology of the femoral intercondylar notch. J Bone Joint Surg Am 89:2150–2155
7. Fayad L, Rosenthal E, Morrison W, Carrino J (2008) Anterior cruciate ligament volume: analysis of gender differences. J Magn Reson Imaging 27:218–223
8. Ferretti M, Ekdahl M, Shen W, Fu F (2007) Osseous landmarks of the femoral attachment of the anterior cruciate ligament: an anatomic study. Arthroscopy 23:1218–1225
9. Fu F, Jordan S (2007) The lateral intercondylar ridge–a key to anatomic anterior cruciate ligament reconstruction. J Bone Joint Surg Am 89:2103–2104
10. Giron F, Cuomo P, Aglietti P, Bull A, Amis A (2006) Femoral attachment of the anterior cruciate ligament. Knee Surg Sports Traumatol Arthrosc 14:250–256
11. Giron F, Cuomo P, Edwards A, Bull A, Amis A, Aglietti P (2007) Double-bundle "anatomic" anterior cruciate ligament reconstruction: a cadaveric study of tunnel positioning with a transtibial technique. Arthroscopy 23:7–13
12. Harner C, Honkamp N, Ranawat A (2008) Anteromedial portal technique for creating the anterior cruciate ligament femoral tunnel. Arthroscopy 24:113–115
13. Kaseta M, DeFrate L, Charnock B, Sullivan R, Garrett WJ (2008) Reconstruction technique affects femoral tunnel placement in ACL reconstruction. Clin Orthop Relat Res 466:1467–1474
14. Kim S, Jung K, Song D (2006) Arthroscopic double-bundle anterior cruciate ligament reconstruction using autogenous quadriceps tendon. Arthroscopy 22: 797.e791–795
15. Lidén M, Sernert N, Rostgård-Christensen L, Kartus C, Ejerhed L (2008) Osteoarthritic changes after anterior cruciate ligament reconstruction using bone-patellar tendon-bone or hamstring tendon autografts: a retrospective, 7-year radiographic and clinical follow-up study. Arthroscopy 24:899–908
16. Nakagawa T, Takeda H, Nakajima K, Nakayama S, Fukai A, Kachi Y, Kawano H, Miura T, Nakamura K (2008) Intraoperative 3-dimensional imaging-based navigation-assisted anatomic double-bundle anterior cruciate ligament reconstruction. Arthroscopy 24:1161–1167
17. Pujol N, Fong O, Karoubi M, Beaufils P, Boisrenoult P (2010) Anatomic double-bundle ACL reconstruction using a bone-patellar tendon-bone autograft: a technical note. Knee Surg Sports Traumatol Arthrosc 18:43–46
18. Shino K, Nakata K, Nakamura N, Toritsuka Y, Nakagawa S, Horibe S (2005) Anatomically oriented anterior cruciate ligament reconstruction with a bone-patellar tendon-bone graft via rectangular socket and tunnel: a snug-fit and impingement-free grafting technique. Arthroscopy 21:1402
19. Siebold R, Ellert T, Metz S, Metz J (2008) Femoral insertions of the anteromedial and posterolateral bundles of the anterior cruciate ligament: morphometry and arthroscopic orientation

models for double-bundle bone tunnel placement–a cadaver study. Arthroscopy 24:585–592
20. Sonnery-Cottet B, Chambat P (2006) Anatomic double bundle: a new concept in anterior cruciate ligament reconstruction using the quadriceps tendon. Arthroscopy 22: 1249.e1241–1244
21. Toritsuka Y, Amano H, Kuwano M, Iwai T, Mae T, Ohzono K, Shino K (2009) Outcome of double-bundle ACL reconstruction using hamstring tendons. Knee Surg Sports Traumatol Arthrosc 17:456–463
22. van Eck C, Lesniak B, Schreiber V, Fu F (2010) Anatomic single- and double-bundle anterior cruciate ligament reconstruction flowchart. Arthroscopy 26:258–268
23. Williams Rr, Hyman J, Petrigliano F, Rozental T, Wickiewicz T (2005) Anterior cruciate ligament reconstruction with a four-strand hamstring tendon autograft. Surgical technique. J Bone Joint Surg Am 87(Suppl 1):51–66
24. Yagi M, Wong E, Kanamori A, Debski R, Fu F, Woo S (2002) Biomechanical analysis of an anatomic anterior cruciate ligament reconstruction. Am J Sports Med 30:660–666
25. Yasuda K, Ichiyama H, Kondo E, Miyatake S, Inoue M, Tanabe Y (2008) An in vivo biomechanical study on the tension-versus-knee flexion angle curves of 2 grafts in anatomic double-bundle anterior cruciate ligament reconstruction: effects of initial tension and internal tibial rotation. Arthroscopy 24:276–284
26. Yasuda K, Kondo E, Ichiyama H, Kitamura N, Tanabe Y, Tohyama H, Minami A (2004) Anatomic reconstruction of the anteromedial and posterolateral bundles of the anterior cruciate ligament using hamstring tendon grafts. Arthroscopy 20:1015–1025
27. Yasuda K, Kondo E, Ichiyama H, Tanabe Y, Tohyama H (2006) Clinical evaluation of anatomic double-bundle anterior cruciate ligament reconstruction procedure using hamstring tendon grafts: comparisons among 3 different procedures. Arthroscopy 22: 240–251
28. Yu J, Garrett WE (2006) Femoral tunnel placement in anterior cruciate ligament reconstruction. Oper Tech Sports Med 14: 45–49
29. Zantop T, Diermann N, Schumacher T, Schanz S, Fu F, Petersen W (2008) Anatomical and nonanatomical double-bundle anterior cruciate ligament reconstruction: importance of femoral tunnel location on knee kinematics. Am J Sports Med 36:678–685
30. Zantop T, Kubo S, Petersen W, Musahl V, Fu F (2007) Current techniques in anatomic anterior cruciate ligament reconstruction. Arthroscopy 23:938–947
31. Zantop T, Wellmann M, Fu F, Petersen W (2008) Tunnel positioning of anteromedial and posterolateral bundles in anatomic anterior cruciate ligament reconstruction: anatomic and radiographic findings. Am J Sports Med 36:65–72
32. Zelle B, Vidal A, Brucker P, Fu F (2007) Double-bundle reconstruction of the anterior cruciate ligament: anatomic and biomechanical rationale. J Am Acad Orthop Surg 15:87–96

Fukui et al. BMC Musculoskeletal Disorders 2010, 11:269
http://www.biomedcentral.com/1471-2474/11/269

BMC
Musculoskeletal Disorders

RESEARCH ARTICLE Open Access

Relationship between radiographic changes and symptoms or physical examination findings in subjects with symptomatic medial knee osteoarthritis: a three-year prospective study

Naoshi Fukui[1*], Shoji Yamane[1], Satoru Ishida[1], Konagi Tanaka[1], Riako Masuda[1], Nobuho Tanaka[1], Yozo Katsuragawa[2], Sakiko Fukui[3]

Abstract

Background: Although osteoarthritis (OA) of the knee joints is the most common and debilitating joint disease in developed countries, the factors that determine the severity of symptoms are not yet understood well. Subjects with symptomatic medial knee OA were followed up prospectively to explore the relationship between radiographic changes and symptoms or physical examination findings.

Methods: One-hundred six OA knees in 68 subjects (mean age 71.1 years; 85% women) were followed up at 6-month intervals over 36 months. At each visit, knee radiographs were obtained, symptoms were assessed by a validated questionnaire, and the result of physical examination was recorded systematically using a specific chart. Correlations between the change of radiographs and clinical data were investigated in a longitudinal manner.

Results: During the study period, the narrowing of joint space width (JSW) was observed in 34 joints (32%). Although those knees were clinically or radiographically indistinguishable at baseline from those without JSW narrowing, differences became apparent at later visits during the follow-up. The subjects with knees that underwent JSW narrowing had severer symptoms, and the symptoms tended to be worse for those with higher rates of narrowing. A significant correlation was not found between the severity of symptoms and the growth of osteophytes. For the knees that did not undergo radiographic progression, the range of motion improved during the follow-up period, possibly due to the reduction of knee pain. Such improvement was not observed with the knees that underwent JSW narrowing or osteophyte growth.

Conclusion: The result of this study indicates that the symptoms of knee OA patients tend to be worse when JSW narrowing is underway. This finding may explain, at least partly, a known dissociation between the radiographic stage of OA and the severity of symptoms.

Background

Osteoarthritis is a common, age-related disorder of the synovial joints, which primarily involves articular cartilage, synovium, and subchondral bones. With increasing longevity, OA has become the most prevalent form of joint disease in developed countries [1]. Knee OA is particularly important in view of its prevalence and association with disability [2,3], which makes this disease a large economic and medical burden to society [1,4].

Pathologically, OA is characterized by focal loss of articular cartilage in weight-bearing areas and new bone formation at joint margins. With the progression of the disease, these changes become apparent on plain radiographs [5-7]. The extent of cartilage loss can be estimated by measuring joint space width (JSW) on radiographs obtained in weight-bearing positions. Newly formed bone tissue is noted as osteophytes at joint margins.

* Correspondence: n-fukui@sagamihara-hosp.gr.jp
[1]Clinical Research Center, National Hospital Organization Sagamihara Hospital, Sakuradai 18-1, Minami-ku, Kanagawa 252-0315, Japan
Full list of author information is available at the end of the article

Knee OA patients most often complained of joint pain, stiffness, restriction of joint motion, and cracking or crepitus within the joints [8]. Among these complaints, joint pain is particularly important because it largely accounts for patients' disability with the disease [3,9,10]. These clinical problems are supposed to arise in association with the above-mentioned pathological changes. However, the severity of a patient's symptoms often does not correlate to the degree of the disease progression evaluated on radiographs [11,12]. In clinics, patients in the early stages of knee OA often have severe knee pain and disability, while those in advanced stages may have only minor symptoms [11,13-17]. Thus, one can not simply assume that the degree of radiographic progression determines the severity of symptoms in knee OA patients.

Knee OA is a highly heterogeneous disease in terms of progression. Previous studies have shown that some OA knees remain stable for years, while others undergo rapid progression [11-13,16,18-21]. Considering this heterogeneity, it may be possible that the patients undergoing disease progression could be clinically distinguishable from those in a stable condition. However, currently it is not known whether the symptoms or physical findings are indeed related to the progression of radiographic changes in knee OA subjects.

To clarify this, we conducted a follow-up study of the subjects with symptomatic knee OA, and investigated the relationship between radiographic progression and symptoms or physical examination findings. The study has revealed several novel aspects in their correlation.

Methods

Subjects

Subjects for this study were recruited at a community medical center from among the patients seeking medical care for symptomatic knee OA. The study was performed under the approval of the institutional review board, and informed consent was obtained in writing from each subject. To be included in the study, the subject had to be 50 years of age or older, in good general health, and have primary knee OA with medial involvement at least in one knee. The persons who had significant impairment in the spine or lower extremities were not requested to participate. The diagnosis of primary knee OA was based on the criteria determined by the American Rheumatism Association with some modifications [8]. That is, the patient had to have persistent knee pain for 3 months or more, and had to have at least one definite osteophyte visible on their radiographs. The involvement of the medial compartment was determined radiographically by the narrowing of the joint space or the presence of a marginal osteophyte in that compartment, with the help of radiographic atlases of knee OA [6,7]. The presence of OA changes in the patellofemoral compartment was not an exclusion criterion, but knees with three-compartmental involvement were not included in the study. A history of a previous injury or surgery was another exclusion criterion. In this investigation, we planned to monitor the progression of the disease primarily by the narrowing of the JSW. For this reason, knees in which the joint space was already obliterated were not eligible for the study. Thus, the inclusion of respective knee joints in the study was finally determined by the radiographs at the enrollment, as described later.

At enrollment, the age, sex, and body mass index (BMI) of the subjects were recorded, and standard blood tests were conducted to determine the serum concentration of C-reactive protein (CRP), erythrocyte sedimentation rate (ESR), and the level of rheumatoid factor. At the enrollment and every 6 months thereafter, radiographs were obtained, and clinical assessment and physical examination were performed repeatedly until the final follow-up at 36 months.

During the study period, all subjects were treated conservatively, although two of them failed to be managed and underwent surgery, as described later. Conservative treatment was started from non-pharmacological therapy that consisted of patient education, muscle strengthening exercise, range of motion exercise, and weight loss when indicated. If the symptoms did not improve, an ointment or patches containing non-steroidal anti-inflammatory drugs (NSAIDs) were prescribed for the subjects. NSAIDs might be given orally to those with severe symptoms. Hyaluronate was administered intra-articularly when the symptoms were intolerable, but corticosteroid was not given to any subjects in this series.

Radiography

At each visit, three radiographs were obtained on each evaluated knee. An anteroposterior (AP) view was obtained in the standing position with the knee in full extension. An axial view was obtained in a 45 degree-flexed position with the subject supine on an X-ray table, following the method of Merchant *et al.* [22] Posteroanterior (PA) radiographs were obtained in the weight-bearing fixed-flexion position with the feet externally rotated 10° and the toes, knees and thighs touching the wall on which the film cassette was placed [23,24]. Before radiography, the outline of the subject's feet was traced on a paper sheet taped to the floor for repositioning the limb in case of repeated exposures. Immediately after the acquisition, parallel alignment of the joint and the x-ray beam was confirmed on each radiograph. When the alignment was poor, the radiograph was taken again after adjusting the tube angle and position.

In the PA radiograph, in particular, the alignment was examined with care: for this radiograph to be acceptable, the tibial spines should be located beneath the femoral notch, and the distance between the anterior and posterior margins of the medial tibial plateau should be equal to or less than 1.5 mm [25]. For the reason mentioned earlier, knee joints whose medial joint space was already closed on the PA radiograph at the enrollment were not included in this study.

Evaluation of radiographs

Progression of OA was determined radiographically by the progression of JSW narrowing and the change in the severity of osteophytosis. In order to evaluate the change of JSW, PA radiographs were converted to digitized images using a laser film digitizer (LD-5500, Konica Minolta MG, Tokyo, Japan), which can scan films at a maximum resolution of a 50-μm focal spot with 256 levels of gray. On these images, JSW was defined as the minimum distance between the femur and tibia in the medial femorotibial compartment. The JSW was measured on the computer system under a proper magnification, which was corrected for magnification by the image of a magnification marker (a steel ball 11 mm in diameter) that was affixed to the lateral aspect of the knee before the acquisition of radiographs.

Severity of osteophytosis was evaluated by the total of severity scores determined at respective sites of the joint on AP and axial view radiographs. On the AP radiograph, formation of osteophytes was rated at the four sites in lateral and medial aspects of the femur and tibia, respectively, using a scale of 0 (absent) to 3 (severest), referring to the standardized radiographic atlases [6,7]. On the axial view radiograph, osteophytes were rated in the same manner at the two sites in lateral and medial aspects of the patellofemoral compartment, referring to the atlas [7]. Thus, the severity of osteophytosis was determined for each knee by the summation of those scores which ranged from 0 (absent) to 18 (severest). These scores were assigned independently by two experienced readers (NF and KT) who were blinded to patient identity or chronological orders. When the score was discordant between them, a third independent reader (YK) made the adjudication on the score in a blinded manner. Inter-reader agreement of the first two readers in the rating was $\kappa = 0.62$ ($p < 0.001$).

Clinical assessment

Symptoms of the patients were evaluated by the Japanese Knee Osteoarthritis Measure (JKOM), a questionnaire designed to evaluate symptoms and functional disabilities with knee OA in the Japanese cultural lifestyle [26]. This is a self-completed questionnaire that consists of a visual analogue scale (VAS) for the degree of global knee pain, and 25 items covering the following four categories: 8 items for pain and stiffness, 10 for conditions in daily life, 9 for general activities, and 2 for health conditions. The overall result was assessed using the result of VAS and the sum of the scores for these 25 items, which ranged from 25 (no complaint) to 133 (possible severest condition).

Physical examination was performed systematically using a specific chart. In the examination, the presence of local warmth in the medial joint space, swelling, tenderness on the medial joint line, crepitation, and range of motion of the joint were examined and recorded. ROM was measured in an assisted-active manner. For this, the subjects were requested to lie supine, and extend or flex each knee as far as possible until discomfort, with the assistance of an examiner, if needed. The knee extension angle and flexion angle were measured and recorded in degrees, respectively, using a large standard goniometer.

Statistical analysis

Statistical significances were determined by Fisher's exact test, and paired or unpaired *t*-test. The relationship between the JKOM score and radiographic progression was analyzed by mixed model analysis, in which the JKOM score and the occurrence of radiographic progression (progression of JSW narrowing or increase in osteophyte score) were included as fixed effects, whereas the follow-up period was entered as a random effect. Receiver operating characteristic (ROC) analysis was employed to determine the predictability of the JKOM score for the occurrence of radiographic progression. The level of significance was set at $P = 0.05$. All analyses were carried out using the SAS statistical software for Windows, version 9.1 (SAS Institute, Cary, NC, USA).

Results

Among the 84 subjects enrolled in the study, 68 completed the 36-months follow-up. There were 10 males and 58 females, with a mean age of 71.1 ± 8.4 and a mean BMI of 25.5 ± 2.5. There were no significant difference in any of the demographic or clinical characteristics between the subjects who were fully followed up and those lost to follow-up (data not shown). In the 68 subjects who completed the follow-up, 30 knees in 30 subjects were not eligible for the study, and the evaluation was performed on the remaining 106 knees. The reasons for the exclusion of the 30 knees were as follows: medial compartment was not the primary site of involvement (14 knees), obliteration of the medial joint space on a PA radiograph (9 knees), tricompartmental involvement (5 knees), history of previous knee surgeries (2 knees). During the follow-up period, prosthetic